DIMENSION REDUCTION BASED ON CENTROIDS FOR MULTIMODAL ANATOMICAL LANDMARK-BASED 3D/2D REGISTRATION OF CORONARY ANGIOGRAMS

Klaus Drechsler and Cristina Oyarzun Laura

Department of Cognitive Computing & Medical Imaging
Fraunhofer Institute for Computer Graphics Research IGD, Darmstadt, Germany

Keywords: Cardiology, Catheterization, Dimension Reduction, 3D/2D Registration, Exhaustive Search, Search Space Reduction.

Abstract: We present an anatomical landmark-based rigid 3D/2D registration algorithm to register computed tomography angiography (CTA) datasets with coronary angiograms (CA) gathered during a cardiac catheterization. It has to solve for six transformation parameters (three rotation and three translation parameters). An exhaustive search in a six dimensional search space is usually computationally very expensive and algorithms using optimization strategies can get lost in local minima. We propose a method based on centroids to reduce search space from six to four dimensions. Modern C-Arm devices store a lot of information about the acquisition geometry that are used to further reduce the search space. We use this method to develop an efficient smart exhaustive search to solve for the six transformation parameters in a competitive time. With our method registration errors of < 2 mm are feasible. Execution times of < 1 sec. can be reached on a QuadCore CPU.

1 INTRODUCTION

The blockage of the coronary arteries, which bring oxygen rich blood to the heart muscle, can lead to damaged/death parts of the muscle. This in turn can lead to a heart attack, which is the leading cause of death worldwide. The current gold standard for detecting these blockages (called plaques) is an invasive coronary angiography. A coronary angiography is the process of injecting a contrast agent directly into the coronary arteries through a catheter and monitoring this process using a C-Arm X-Ray device that is able to record the injection as a video sequence.

We assume that in the near future the diagnostic of the coronary arteries will be done using non-invasive computed tomography angiography (CTA) and that only the intervention, if necessary, will be done in a catheter laboratory (to insert e.g. stents) or in an operation room (to do a bypass surgery). This assumption is not unrealistic: A steadily increasing number of hospitals are already using CTA for diagnostic purposes and papers successfully investigating CTA for this use case were published (e.g. (Hoffmann et al., 2005) and (Mieres et al., 2007)). A combina-

tion of preoperatively gathered CTA dataset and operatively gathered CA will further enhance the trust in CT for the assessment of the coronary arteries. We use a tool that is able to carry out an automated quantitative analysis of the coronary arteries using CTA datasets (Wesarg et al., 2006), whose output has been positively evaluated in a clinical study (Khan et al., 2006), (Wesarg et al., 2008). Our goal is to display the analysis results of this tool (the found pathologies like plaques) directly in the CA of the patient. Thus, the problem can be reduced to a 3D/2D rigid registration problem. It has to find three rotation and three translation parameters that bring the 3D CTA volume into a position within a virtual C-Arm device that equals the position of the patient on the table when the 2D CA was gathered using the real C-Arm device. A virtual CA gathered by the virtual C-Arm device is then approximately the same than the CA gathered by the real C-Arm device.

In this paper we present a landmark-based 3D/2D registration algorithm to register CTA datasets with CAs. Therefore the CTA is used to generate an artificial CA, called digitally reconstructed radiographs (DRR), which is used in an intermediate step and dis-

played side-by-side with the CA to allow the user to select anatomical correspondences. Afterwards an exhaustive search is executed to solve for the six parameters (three rotation and three translation parameters). We introduce a novel method to reduce the search dimension from six degrees of freedom to four, which to the best of our knowledge has never been applied to this problem before. Although we used this method to speed-up an exhaustive search algorithm, it can be also used with more advanced optimization strategies. However, compared to other methods an exhaustive search does not get lost in local minima. We show in an experiment that RMS registration errors of < 2 mm are feasible and execution times of less than 1 sec. can be reached on a QuadCore CPU.

The remainder of this paper is organized as follows. The next section presents related work. The following section 3 describes the workflow of the registration process from an user point of view. In section 4 the used methods are described. Especially our registration and dimension reduction methods are detailed. In section 5 the results of an experiment are presented and discussed in section 6. And in section 7 we finally conclude this paper.

2 RELATED WORK

When developing applications that combine and use information gathered from different modalities, registration plays an important role. 3D/2D registration algorithms can be classified as intensity-based, feature-based or as hybrid approaches between those two. Feature-based methods can be further classified according to the type of feature used.

A system that uses external features is described by Filippatos in (Filippatos, 2006). They use a fiducial-based registration to match the 3D CT volume to the intraoperative x-ray image. Therefore they calculate the transformation matrix that matches the 3D points (that correspond to fiducial markers in the CT volume) with the corresponding 2D x-ray points and use it to initialize the 3D volume in an adequate position.

The work presented in (Lau and Chung, 2006) uses internal features. They studied how to avoid the problem of local minima that occurs in high-dimensional image registration. For their experiments they used the vessels centerline as feature. The optimization method consist of calculating the result of the cost function in a low resolution environment, optimizing it with Powells method using sum of squared differences as metric, and doing a final optimization with the best obtained transformation matrix in the

high resolution environment. The authors report an execution time of 13 min. on one 2.5 GHz processor with 512 GB RAM using Matlab. They estimate that they can achive an execution time of approximately 30 sec. using C++ and further optimizations.

In (Langs et al., 2004) the authors describe a registration method based on internal features. In their registration approach the user has to mark two corresponding points in the 3D model of the vessels and the 2D x-ray image. However, if a doctor has to select a point in 3D and a corresponding point in 2D then he has either to reconstruct a 3D image from the 2D x-ray or a 2D image from the 3D model in his head to decide which points correspond. We avoid this by generating a DRR from the CT-data and let the user select the point in two similar 2D images. The authors report execution times of approximately 0.3 sec. Unfortunately it is not clear how they solved for the six transformation parameters. It seems that they use the primary and secondary angle of the C-Arm device together with two manually selected points to directly solve an equation to get the remaining parameters. But because of patient movement between acquisitions and error-prone points this seems not the way to go.

In (Groher et al., 2007) the authors propose an automatic 3D/2D registration algorithm based on bifurcations as internal features. They use shape context descriptors to establish correspondences between bifurcations in both modalities. The authors used a rigid phantom for their experiment and reached an execution time of 2-6 sec. for the registration.

The work presented in (Turgeon et al., 2005) belongs to the class of intensity-based methods. It deals with similarity-based 3D/2D registration of coronary angiograms using binary images instead of gray scale images. The authors obtain a 4D model of the heart composed of realistic 2D and 3D images to create a simulation environment for evaluation purposes. The registration is carried out using entropy correlation coefficient as metric and the downhill simplex method as optimization strategy. The execution time of their algorithm is between 17 and 32 sec. on two 3 GHz Xeon processors with 1 GB of RAM.

3 APPLICATION WORKFLOW

In this section the workflow from a user point of view is described. We assume that the C-Arm is calibrated and that the intrinsic parameters are known. Basically the workflow consists of six consecutive steps as follows.
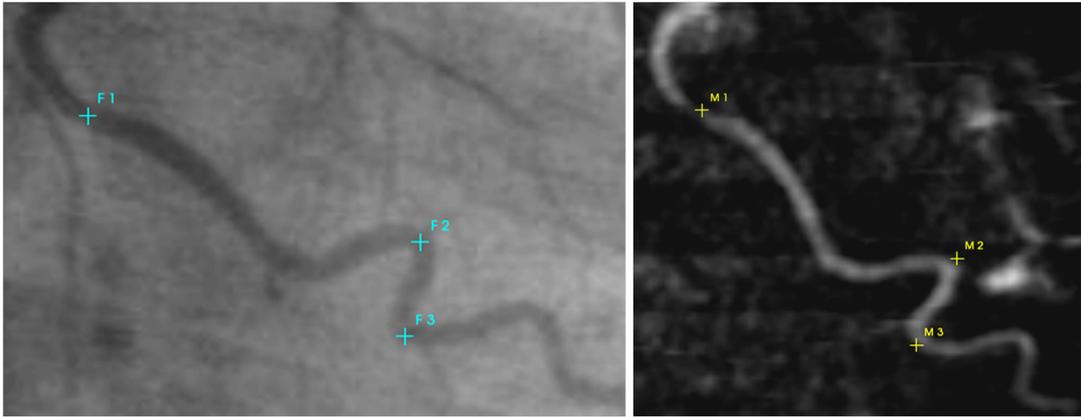
Figure 1: The coronary angiogram and a DRR calculated from CT data is displayed. The user user has to select corresponding landmarks in both images.

Step 1 - Image Selection. As described in the introduction section, during the catheterization a video sequence of the process is recorded. In the first step an appropriate image from this sequence has to be selected. An image is considered as appropriate if the displayed heart cycle corresponds to the heart cycle in which the CTA data was gathered and if the injected contrast agent is still in the arteries. Using available ECG information, this is not difficult to do.

Step 2 - DRR Creation. The task of the next step is to create a DRR from the CTA dataset that shows the heart approximately in the same position as the heart in the CA that was selected in step 1. State-of-the-art angiographic C-Arm devices store lots of information, including the rotational angles of the C-Arm during the recording of the video sequence. This information is used to create the DRR. However, older C-Arm devices do not store all rotational angles, so that user intervention would be necessary to approximately find the missing angles.

Step 3 - Display DRR and CA. In this step the created DRR and CA are displayed side-by-side on two monitors (see fig. 1) or overlapped on one monitor. In the latter case the user can crossfade the two images using a slider.

Step 4 - Select Corresponding Point Pairs. In this step the user has to select n corresponding anatomical landmarks in both images as depicted in fig. 1. Typically $n = 4$ is sufficient, but more points can improve the quality of the final result.

Step 5 - Align Points. After the user has selected n corresponding landmarks, the points in the DRR image will be automatically aligned to the closest vessel centerline. This enables the backprojection of the selected 2D DRR points to 3D space of the CTA volume, which is required to carry out a 3D/2D landmark-based registration. Therefore we developed a concept that we call 'alignment map'. The 3D centerline voxels are projected into 2D space with the same parameters used for creating the DRR. The alignment map contains the projected 2D points and the corresponding 3D points of the centerline. The effect of aligning the points is shown in fig. 2. After aligning the points, they can be backprojected to 3D space by querying the alignment map.

Step 6 - Carry out Registration. At this point the following parameters are given.

- n corresponding 2D points $(a_i, d_i), i : 0...n-1$

- 3D points $D_i = map(d_i)$ (using the alignment map)

- Matrix K with intrinsic parameters of the C-Arm device, which includes the focal length which can be found as source-to-detector distance $dist_{std}$ which can be found in the DICOM header

- Primary (γ) and secondary (α) angles found in the DICOM header

- The source-to-object distance $dist_{sto}$ found in the DICOM header

Given these parameters the problem can be formulated as follows. Find euler angles α, β, γ and $t = (t_x, t_y, t_z)$ such that

$$a_i = K \cdot (R_{\alpha, \beta, \gamma} \cdot D_i + t) \tag{1}$$

Because the selected corresponding landmarks are error-prone and not exact the problem turns out to be a minimization problem.
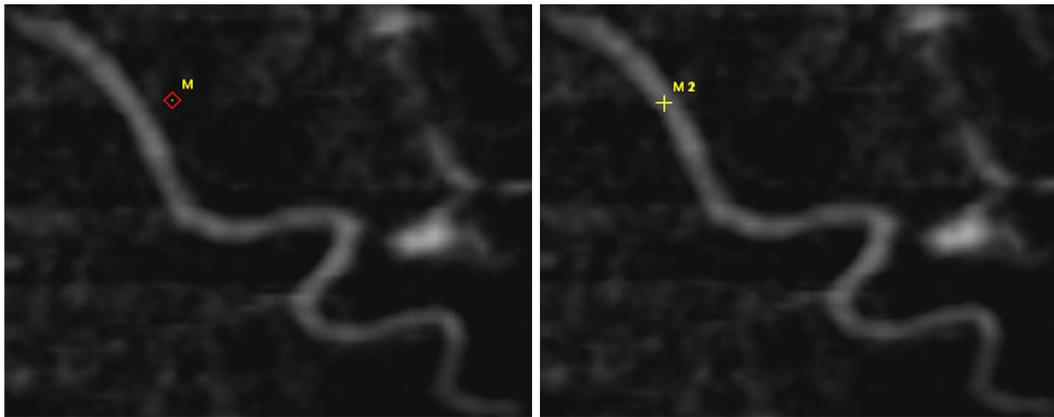
Figure 2: The selected point in the left image is aligned to the closest vessel centerline as shown in the right image. This enables the backprojection of this 2D point into 3D space using our alignment map. The images show an extreme example to illustrate the idea. Usually points are selected that are somewhere on a vessel or at least very close to it and not that far away.

4 METHODS

The following subsection gives an overview of used algorithms to extract the heart, segment arteries and generate DRRs. Afterwards our registration method is described.

4.1 Image Processing

Cardiac CT data normally contains non-cardiac structures such as ribs, lungs or the sternum. These structures obscure the view to the heart, but an isolated heart is necessary to make a visualization of the coronary arteries on the surface of the heart possible. We use the approach presented in (Jaehne et al., 2008) which is desribed as follows. A partition (labels) of the anatomical structures by automatically selecting thresholds using Otsus method (Otsu, 1979) is obtained. The two brightest gray levels are used to calculate the center of gravity for every axial slice, which lies in the middle of the heart. From this point radial search rays are send out in order to find the outer boundary of the heart. These rays will be too long at places where overlapping structures like the aorta or the sternum are present, thus preventing this method to function properly. These parts are handled as follows. On each side of the aorta and the sternum the last rays which hit lung tissue and therefore have the correct length are automatically detected. Interpolation is then used to correct the rays between them. The found end points are connected and a binary mask is generated which is used as a mask on the original CT data to extract the heart.

The result of the previous algorithm is used to segment the coronary arteries using a tracking based segmentation algorithm, which is described in (Wesarg and Firle, 2004). The data is preprocessed with an adaptive threshold filter that takes the gray values of three user provided seed points (start, direction and end point) and the CT data as inputs. It takes into account that the contrast agent is not equally distributed in the vessel. It follows an opening operation to remove connections to neighboring tissues and to the vessel wall behind hard plaques. The actual algorithm gets the results of the opening operation, the original image and the output of the adaptive threshold filter to calculate a path (centerline and border) between a start and end point that lies within the vessel. Afterwards a 3D model is generated using the marching cubes algorithm (Lorensen and Cline, 1987).

We use the approach presented in (Lacalli et al., 2008) to calculate a DRR of the heart. First a preprocessing of the original CT data is carried out to avoid insufficient results due to non-cardiac structures and large cardiac cavities (e.g. ventricles and atria) that are filled with contrast agent. The latter would occlude the coronary arteries in the DRR and must therefore be removed. To remove the cavities from the extracted heart a thresholding operation on the labeled CT data (that was generated in the heart extraction step described above) is first applied to remove everything but the highest label that correlates with both the cavities and the arteries. The coronary arteries are then removed by an erosion operation followed by a neighborhood filter along all the three orthogonal axes. Finally a dilation operation is applied to restore the original size of the cavities. The result is used as a mask to remove the cavities from the extracted heart. A perspective projection is then carried out to generate the DRR to simulate a coronary angiogram.

4.2 Registration Method

As written in the previous section, we are dealing with a minimization problem. We use the root mean square (RMS) error as metric that we are minimizing using our algorithm. The RMS error is defined as

$$RMS_{error} = \sqrt{(a_i - d_i')^2} \qquad (2)$$

where a_i is the selected point in the CA and d_i' the transformed and projected point D_i calculated according to equation 1 as

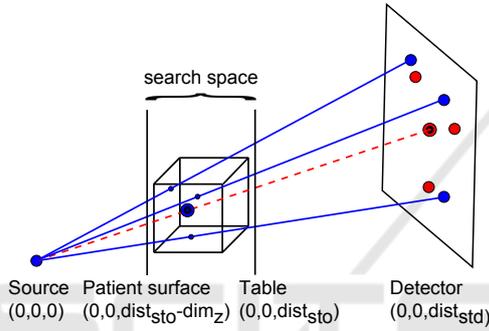$$d_i' = K \cdot (R_{\alpha,\beta,\gamma} \cdot D_i + t) \qquad (3)$$

Figure 3: The image shows the most important ideas to reduce the dimensions and search space. The blue points in the cube are the points D_i'. The red line is the centroid line from source to the centroid of the points a_i. The search space is limited by the table and the patient surface.

We developed an algorithm that we call 'smart exhaustive search' that guarantees to find the minimum RMS_{error} (because it does an exhaustive search) and is very well parallelizable. A normal exhaustive search has to take six degrees of freedom into account and thus would be very inefficient for our application. The key idea behind our algorithm is to reduce the dimensions to four degrees of freedom (three rotation and one translation parameter) and then further reduce the remaining search space by taking all the given parameters into account.

We explain now how we reduced the degrees of freedom from six to four. Therefore we define that the source of the C-Arm device is always at the origin of the world coordinate system and the detector plane is $dist_{std}$ away in the z-dimension, thus $src = (0,0,0)$ and $det = (0,0,dist_{std})$. We further define the centroid of the n 2D points a_i as

$$centroid_{2D} = \begin{pmatrix} c2d_x \\ c2d_y \end{pmatrix} = \frac{1}{n} \sum_i^{n-1} a_i \qquad (4)$$

The result of equation 4 is enhanced by a z-component, which is set to the source-to-detector distance $dist_{std}$, thus $centroid_{2D}$ is guaranteed to lie on the detector plane:

$$centroid_{2DZ} = \begin{pmatrix} c2d_x \\ c2d_y \\ dist_{std} \end{pmatrix} \qquad (5)$$

Next we construct a line, called centroid line or *cline*, from the source of the C-Arm device to $centroid_{2DZ}$ (see red dotted line in fig. 3), which is given by

$$cline(p) = \begin{pmatrix} t_x \\ t_y \\ t_z \end{pmatrix} = src + p \cdot (centroid_{2DZ} - src) \quad (6)$$

Parameter p has to be between 0 and 1 and indicates the distance from src in direction of det. Further, we define the rotated and translated points D_i as

$$D_i' = (R_{\alpha,\beta,\gamma} \cdot D_i + t) \qquad (7)$$

and equally to equation 4 the centroid of the n 3D points D_i' as

$$centroid_{3D} = \begin{pmatrix} c3d_x \\ c3d_y \\ c3d_z \end{pmatrix} = \frac{1}{n} \sum_i^{n-1} D_i' \qquad (8)$$

Now it can be observed that, after a successful registration, in the theoretical case where the given landmarks are accurately known, the centroid of D_i' must lie on $cline(p)$ and $K \cdot centroid_{3D} = centroid_{2DZ}$ (see fig. 3). We can then calculate the resulting translation vector t from parameter p using equation 6. This knowledge can be used to reduce the degrees of freedom from six to four by moving $centroid_{3D}$ during the exhaustive search along $cline(p)$, thus we only have to solve for four parameters, namely α, β, γ and p to minimize equation 2. In practice the landmarks are not accurately known, but error-prone. The effect of moving $centroid_{3D}$ along $cline(p)$ in this case is that the error between corresponding landmarks is averaged.

We further reduce the search space by taking the source-to-object distance $dist_{sto}$ and the physical dimension in z-direction dim_z of the CT volume into account. The name 'source-to-object' is a little bit misleading. It is really the distance between the source of the C-Arm device and the table where the object (the patient) is laying on. Thus, equation 2 is minimal when $centroid_{3D}$ lies on $cline(p)$ somewhere between the table at coordinates $(0,0,dist_{sto})$ and the patient surface at coordinates $(0,0,dist_{sto} - dim_z)$ (see fig. 3).

197

Table 1: Summary of the used parameters.

Parameter	α	β	γ	dim_z	$dist_{sto}$
Value	0.1	n/a	-30.9	300	700

The search space can be reduced even more by taking the given angles α and γ into account. Even if the values are accurately known, the patient is not lying in the same position as he was during the CTA acquisition. Thus, these values can only be used as rough estimations. In (Byrne et al., 2004) the authors searched ± 8 degrees around the given values. We found that for our dataset searching ± 20 degrees around the stored values is necessary to find the minimal RMS_{error}. Thus, this value varies between different C-Arm devices and different CTA/CA pairs.

4.3 Parallelization

The described method can be parallelized using n processors by dividing parameter p into n equal sized parts and let each processor execute independently the described method for one part. Then, the processor that calculated the smallest RMS_{error} has found the solution.

5 RESULTS

We evaluated our algorithm with one CTA/CA dataset pair. The analysis tool mentioned in the introduction that we use to analyze the coronary arteries is able to segment single branches of the coronary artery tree and to calculate the vessel centerline. To qualitatively verify the registration results, we overlaped these centerlines with the CA. We searched ± 20 degrees around all given angles and around 0 for β. We repeated the experiment two times. The first time with a step width of 1 (experiment A), the second time with a step width of 2 (experiment B). Therefore we modified equation 6 by normalizing the vector $centroid_{2DZ} - src$. With this modification parameter p has to be between 0 and the length of $centroid_{2DZ} - src$ before normalization. All experiments were executed on a PC equipped with an Intel 2.5 GHz DualCore CPU, 4 GB RAM and Windows 7 x64 as operating system. Table 1 summarizes the parameters we used for the registration.

The registration was done using the workflow described in section 3 and repeated four times using four to seven corresponding point pairs. The results are presented in table 2 and 3. For qualitative evaluation we overlapped the centerlines of two segmented branches of the coronary arteries in the CTA dataset

Table 2: Quantitative results of experiment A using a step width of 1 mm.

Landmarks pairs	4	5	6	7
RMS error [mm]	0.81	0.76	1.16	1.5
SingleCore [s]	23.1	24.9	28.0	32.8
QuadCore [s]	5.8	6.2	7.0	8.2

Table 3: Quantitative results of experiment B using a step width of 2 mm.

Landmarks pairs	4	5	6	7
RMS error [mm]	0.83	0.78	1.2	1.54
SingleCore [s]	1.8	1.9	2.0	2.4
QuadCore [s]	0.45	0.48	0.5	0.6

with the CA. The results are shown in fig. 4. There were no visible differences between experiment A and B. The estimated values for a QuadCore CPU were calculated by dividing the execution time on a SingleCore CPU by four.

6 DISCUSSION

A general problem for methods based on the vessel centerline as feature is that they rely on good vessel segmentation algorithms which in turn depend on good datasets where the contrast agent is spread optimally. This is also the case with our method. We had three CTA/CA dateset pairs and were only able to apply our method to one pair. The reason was mainly that the contrast agent was not very well visible in the CT datasets.

There is no visible and measurable difference between the top two images of fig. 4, but a short part of the overlapped vessel centerlines is cleary not overlapped correctly near the root of the coronary artery tree. In the bottom two images this problem is reduced by selecting more point correspondences at the cost of slightly misalignments at other places of the vessel tree. Although the RMS error was greater for the bottom images, they generally look better than the images in the top row. This is due to the fact that the calculated centroids average landmark errors during the registration process.

Because we manually selected a frame from the recorded angiography, it could be that we selected one that was not the best choice, hence the misalignments. But using ECG information this should not be a problem in general. Another reason could be that the manually selected points were not corresponding very well and thus introducing an error in the registration process.

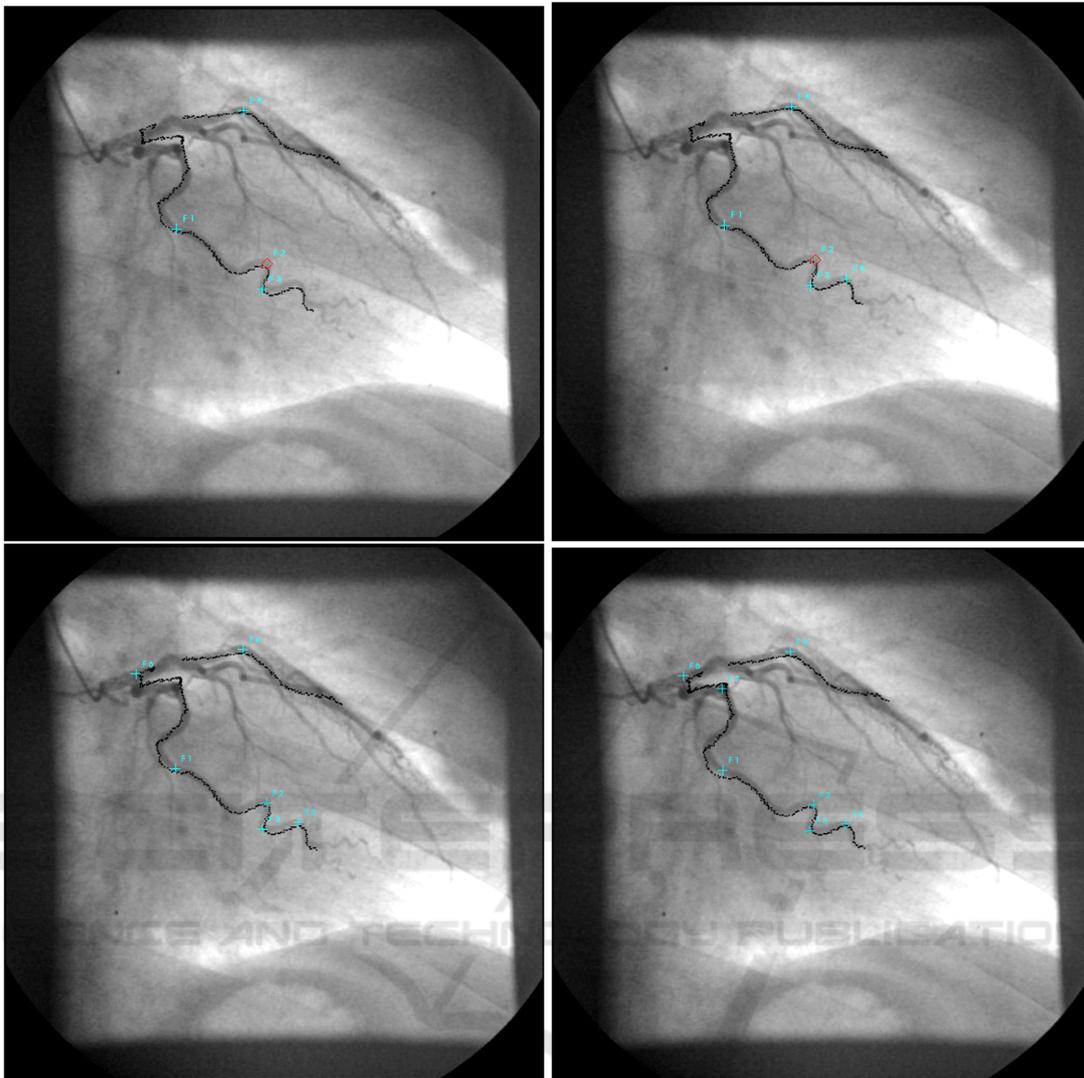The manual selection of corresponding points is

Figure 4: Qualitative results with four (top left), five (top right), six (bottom left) and seven (bottom right) manually selected corresponding point pairs.

currently the biggest disadvantage of our method. An interesting approach to solve for this can be found in (Groher et al., 2007). The authors developed a method to automatically find corresponding bifurcations in 2D and 3D images based on shape context descriptors.

There were no significant visible differences between experiment A and B, but using a step width of 2 in experiment A is significant faster.

In other experiments we found that it is important which landmarks are chosen. If only landmarks from one vessel branch are chosen, then it is likely that the other branches will be fairly misaligned. This can be acceptable if only one branch is of interest. But in general it can be said, as a rule of thumb, that as

much landmarks as possible should be spread over the whole vessel tree. Fortunately, the process of selecting corresponding landmark pairs is quite easy and fast.

As can be seen from table 2 and 3 the processing time needed to solve for the six transformation parameters is, thanks to the presented strategies to reduce the dimensions and search space, quite competitive when taking the estimated times into account. If faster processing times are needed, the exhaustive search can be replaced by more advanced optimization strategies at the cost of risking to get lost in local minima. Another option would be to use more processors for the calculation and/or specialised architectures like CUDA.

7 CONCLUSIONS

We presented a novel dimension reduction method based on centroids that we successfully applied to a multimodal anatomical landmark-based 3D/2D registration problem. We used this method to speed-up an exhaustive search to solve for the six transformation parameters. In an experiment we have shown that this method produced good results with competitive processing times. The presented dimension reduction technique is not limited to exhaustive search, but can also be used in combination with optimizers to speed-up feature-based 3D/2D registration problems, where features represents anatomical landmarks like e.g. branch points.

Future work includes the automated detection of corresponding point-pairs as inspired by (Groher et al., 2007) and the use of more advanced optimization strategies together with the presented dimension reduction method to further speed-up the registration for real-time usage. Furthermore, we are thinking about ways to take the complete vessel centerlines into account to improve the registration results.

REFERENCES

Byrne, J. V., Colominas, C., Hipwell, J., Cox, T., Noble, J. A., Penney, G. P., and Hawkes, D. J. (2004). Assessment of a technique for 2d-3d registration of cerebral intra-arterial angiography. *The British Journal of Radiology*, 77(914):123–128.

Filippatos, K. (2006). A navigation tool for the endovascular treatment of aortic aneurysms - computer aided implantation of a stent graft. Master's thesis, Technical University of Munich.

Groher, M., Hoffmann, R.-T., Zech, C. J., Reiser, M., and Navab, N. (2007). An efficient registration algorithm for advanced fusion of 2d/3d angiographic data. In *Bildverarbeitung fr die Medizin (BVM)*, pages 156–160. Springer.

Hoffmann, M. H. K., Shi, H., Schmitz, B. L., Schmid, F. T., Lieberknecht, M., Schulze, R., Ludwig, B., Kroschel, U., Jahnke, N., Haerer, W., Brambs, H.-J., and Aschoff, A. J. (2005). Noninvasive coronary angiography with multislice computed tomography. *JAMA: Journal of the American Medical Association*, 293(20):2471–2478.

Jaehne, M., Lacalli, C., and Wesarg, S. (2008). Novel techniques for automatically enhanced visualization of coronary arteries in msct data and for drawing direct comparisons to conventional angiography. In *VISIGRAPP 2008: International Joint Conference on Computer Vision and Computer Graphics Theory and Applications. Proceedings. CD-ROM.*, pages S.290–296. INSTICC Press.

Khan, M., Wesarg, S., Gurung, J., Dogan, S., Maataoui, A., Brehmer, B., Herzog, C., Ackermann, H., Assmus, B., and Vogl, T. (2006). Facilitating coronary artery evaluation in mdct using a 3d automatic vessel segmentation tool. *European Radiology*, 16(8):1789–1795.

Lacalli, C., Jaehne, M., and Wesarg, S. (2008). Automatisierte verfahren zur verbesserten visualisierung der koronararterien in msct-daten und fuer die direkte vergleichbarkeit zur angiographie. In *Bildverarbeitung fuer die Medizin 2008: Algorithmen - Systeme - Anwendungen*, pages 283–287.

Langs, G., Radeva, P., Rotger, D., and Carreras, F. (2004). Building and registering parameterized 3d models of vessel trees for visualization during intervention. In *ICPR '04: Proceedings of the Pattern Recognition, 17th International Conference on (ICPR'04) Volume 3*, pages 726–729, Washington, DC, USA. IEEE Computer Society.

Lau, K. and Chung, A. (2006). A global optimization strategy for 3d-2d registration of vascular images. In *BMVC06*, volume 2, page 489ff.

Lorensen, W. E. and Cline, H. E. (1987). Marching cubes: A high resolution 3d surface construction algorithm. *SIGGRAPH Comput. Graph.*, 21(4):163–169.

Mieres, J. H., Makaryus, A. N., Redberg, R. F., and Shaw, L. J. (2007). Noninvasive cardiac imaging. *AFP: American Family Physicians*, 75(8):1219–1228.

Otsu, N. (1979). A threshold selection method from gray-level histograms. *IEEE Transactions on Systems, Man and Cybernetics*, 9(1):62–66.

Turgeon, G.-A., Lehmann, G., Guiraudon, G., Drangova, M., Holdsworth, D., and Peters, T. (2005). 2d-3d registration of coronary angiograms for cardiac procedure planning and guidance. *Medical Physics*, 32(12):3737–3749.

Wesarg, S. and Firle, E. A. (2004). Segmentation of vessels: The corkscrew algorithm. In *Medical imaging 2004: Image processing.*, volume 5370, pages 1609–1620.

Wesarg, S., Khan, M., Jaehne, M., and Lacalli, C. (2008). Automatisierte analyse der koronararterien basierend auf msct-daten. *Deutsche Zeitschrift fuer klinische Forschung*, 11(3/4):28–33.

Wesarg, S., Khan, M. F., and Firle, E. (2006). Localizing calcifications in cardiac ct data sets using a new vessel segmentation approach. *Journal of Digital Imaging*, 19:249–257.